The Application of Computational Fluid Dynamics to Sails

Arvel Gentry
The Boeing Company
Seattle, Washington

Proceedings of the Symposium on Hydrodynamic Performance Enhancement for Marine Applications, Newport, Rhode Island, October 31 - November 1, 1988

Abstract

This paper presents examples of the application of Computational Fluid Dynamics (CFD) in understanding the aerodynamics of sails. The basic principles of the generation of lift and the jib-mainsail slot effect for thin soft sails are reviewed. The application of this technology to the 12-Meter yacht mast design problem is presented. The paper concludes with an experimental study of the use of CFD techniques in understanding the design problems of a multi-element solid-wing sail.

Nomenclature

C_ℓ	= section lift coefficient
C_L	= wing lift coefficient
$C_\ell c/c_{ref}$	= span load coefficient
c	= local chord
c_{ref}	= reference chord
Cp	= surface pressure coefficient $(p-p_\infty) / (1/2\rho V_\infty^2)$
	$= 1 - (V/V_\infty)^2$
H	= boundary layer shape factor - δ^*/θ
p	= surface pressure
p_∞	= freestream static pressure
Re	= Reynolds number per foot
S	= stagnation streamline
V	= local surface velocity
V_∞	= freestream velocity
X	= longitudinal distance
X_{sep}	= location of separation point
Y	= span location and airfoil y-coordinate
α	= angle of attack
ρ	= air density
δ^*	= boundary layer displacement thickness
θ	= boundary layer momentum thickness

Introduction

The digital computer plus advanced mathematical techniques has spawned a relatively new and powerful field of aerodynamics called Computational Fluid Dynamics (CFD). In its simplest terms, CFD is the process of taking a physical flow problem, breaking it down into a suitable set of equations, and solving them on a digital computer. The use of CFD in the aircraft design process has steadily grown over the past twenty years and has also seen some application to the aerodynamics of sails over that same time period.

Before the digital computer, aerodynamicists relied on basic theory supplemented by extensive wind tunnel and flight testing. However, the approximations present in wind tunnel testing and the high cost of both tunnel and flight tests slowed the design process. In physical testing, all flow phenomena are present so that the real effects are seen within the limitations of the experiment. However, in physical testing it is usually difficult to separate the various effects so that the real cause and effects of the physics can be understood.

By its very nature, CFD is able to probe such problems. Within the computer it is possible to test the sensitivity of the mathematical assumptions and the physical processes that they simulate. The computer even provides a means of discovering new physical phenomena. In this sense, CFD is closer to experimental than to theoretical fluid dynamics. However, just as with experimental fluid mechanics, CFD has its own difficulties and limitations.

Present day codes are becoming quite sophisticated. Everyday production tools for subsonic work such as higher order panel methods, three-dimensional boundary layer methods, and inviscid-viscous coupled solutions, have provided unique insights into basic aerodynamic problems. The future looks even brighter with the more powerful Euler methods with coupled boundary layer solutions. The application of the ultimate, the solution of the Navier-Stokes equations, is becoming practical for increasingly complicated geometric shapes, but requires more computer speed, memory and cost than is presently available to someone doing avocational research in sail aerodynamics. This paper will, therefore, limit itself to the use of the more basic tools based on panel methods plus boundary layer solutions.

The application of CFD to sails has provided several advantages over testing. With CFD we can separate and identify the physical phenomena involved. The application of CFD is much cheaper than testing, providing one has access to the appropriate computer programs and a powerful computer. The disadvantages are that CFD is only as good as the mathematical equations and assumptions used in representing the physical flow.

© 1900 Arvel Gentry

Also, all CFD codes require the precise input of the geometry of the shapes to be studied. In the case of soft thin sails, this is difficult. Under sail, the crew can adjust the sails precisely to the flow conditions, but this is difficult to accomplish in a computer program.

This paper presents the experiences of the author in exploring the use of CFD on sailing problems over a number of years. Early explorations were quite significant in that they led to the correct explanation for the jib-mainsail interaction problem (the slot effect). CFD technology also was applied to the problems of mast cross-section shape design for America's Cup l2-Meter yachts. This paper reviews this earlier work on thin soft sails and concludes with some results from an experimental study of the use of the latest CFD techniques on a solid-wing sail such as used on high-performance catamarans.

Aerodynamics of Sail Interaction

In 1973, *SAIL* magazine published the first of a series of articles by the present author on the aerodynamics of sails (1, 2). These articles were based on research reported in 1971 (3). An updated version of this material was presented in (4). The basic objective of these references was to understand how two sails, the jib and mainsail, interact with each other (the "slot" phenomena). The accepted explanation was that the slot between the two sails caused a high-speed venturi effect and that it "energized" the boundary layer on the lee side of the mainsail and kept it from stalling. This popular explanation in the sailing literature followed the then current description for the wing/slat interaction problem in the aerodynamic literature. Both were wrong. The use of CFD provided the correct answers.

The author's co-workers in the early 70's had developed a new multi-element CFD code (5) and were beginning to gain new insights into high-lift design problems. It seemed clear that these same concepts must apply to the sail interaction problem. With the new CFD code it was possible to separate the various phenomena and to gain a new understanding of the physical problem.

The Generation of Lift

The fundamental problem as to how a surface such as a sail generates lift is rather difficult to understand for the average non-technical sailor. The fact that it is the viscosity of air that makes lift possible is even more difficult to grasp. The concepts used in CFD codes help in explaining the principles involved as illustrated in Figures 1 through 3.

Early versions of these illustrations were generated by the author using an analog field plotter, an early and simple CFD method (3). Later the streamlines were determined more accurately using a potential flow program for two-dimensional airfoils (5). This program was probably typical of the state-of-the-art at the time (1965). However, it contained no viscous interaction or separation flow modeling capabilities. The method was based on the use of a distribution of source density over the surface. Applying the condition of zero normal velocity on the surface gave an integral equation for the source distribution. The integral equation was replaced by a set of linear algebraic equations for the values of the source density on the elements. Once these were solved for the source distribution, all flow quantities of interest (velocity, pressure, etc.) could be calculated. The body surface was approximated by a large number of small surface segments or elements, over each of which the source density was assumed constant. Specification of the trailing edge flow condition (the Kutta condition) could be turned on or off.

Figure 1 shows what the flow about a simple airfoil would look like if the air had no viscosity. This is easily simulated with the potential flow program by turning off the Kutta condition. Without viscosity the flow would make the turn at the trailing edge as shown in Figure 1, the streamlines would be symmetrical and there would be no lift and no drag.

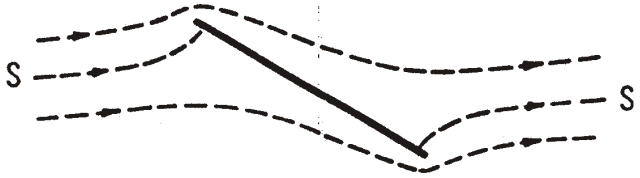

Figure 1. Flow if air had no viscosity.

The real air does have viscosity but its primary effect is near the surface of an object (the boundary layer). The thickness and characteristics of this layer depend upon how it is treated by the external flow and in particular, by the pressure gradient. A rapidly increasing pressure will thicken the boundary layer and eventually cause it to separate from the surface. For the flow in Figure 1, the boundary layer would not be able to withstand the rapid increase in pressure around the trailing edge. It would separate and shed the starting vortex as shown in Figure 2.

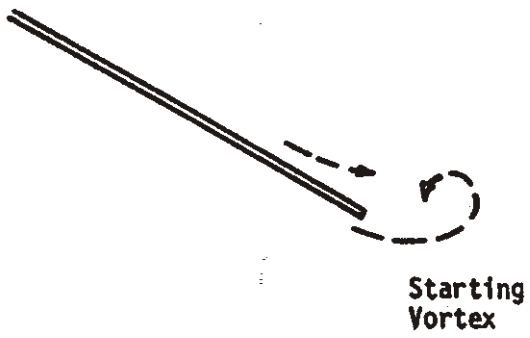

Figure 2. Formation of starting vortex at the trailing edge.

Once we know what happens at the trailing edge we can adapt our mathematical representations of the flow and produce useful answers. The condition of flow leaving the trailing edge, the Kutta condition, certainly has been understood for many years. In theoretical aerodynamics, the Kutta condition is satisfied by imposing a mathematical circulation about the airfoil until the flow leaves the

trailing edge smoothly. With the Kutta condition imposed, the viscous effects can then be neglected and the mathematical tool used to explore and understand the flow about shapes without separation. The resulting final flow with the Kutta condition imposed is shown in Figure 3. The airfoil now generates lift.

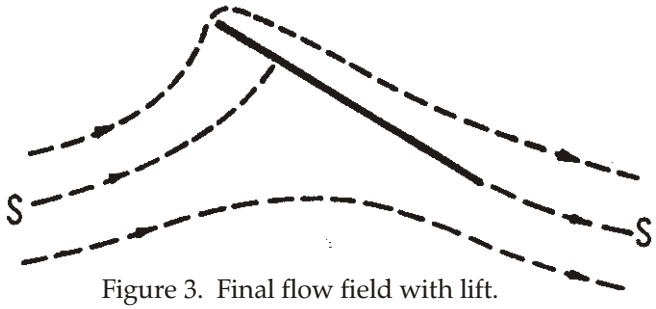

Figure 3. Final flow field with lift.

Although the circulation about the airfoil as generated in theoretical aerodynamics and as simulated by potential flow programs seems like just a mathematical trick, this is not the case. The circulation is real and can be viewed by a simple experiment using a bathtub with about two inches of water (4). A small airfoil is placed at one end of the tub and then moved smoothly toward the other end. This will cause the formation of the starting vortex as the viscosity takes over and forces a Kutta condition at the trailing edge. After a short distance, the flow will adjust and there is an upwash in front of the airfoil and a downwash behind. If the airfoil is then removed from the water an additional vortex is left behind. This is the circulation required to satisfy the Kutta condition and its magnitude determines the amount of lift generated by the airfoil.

Jib/Mainsail Interaction

When two airfoils are close to each other such as with the jib and mainsail, then two circulation fields are present, Figure 4. We may easily deduce a number of things from this figure. It is clear that the two circulations oppose each other in the slot between the jib and mainsail. The air speed in this region will be slowed down. The two circulations should add to each other in the area to the lee side of the jib. In front of the jib, the two circulations should add together to increase the jib upwash. If no flow separation is present, the Kutta condition must be satisfied at both the mainsail and jib trailing edges.

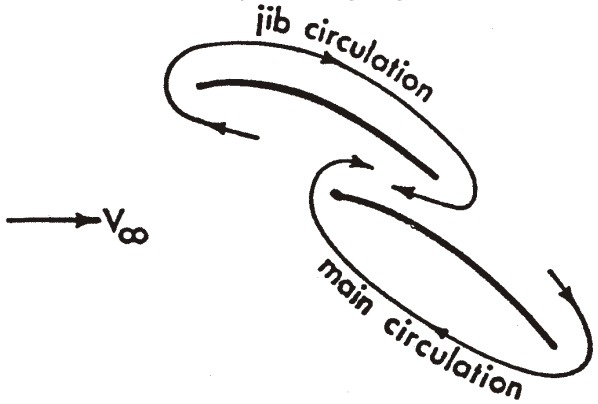

Figure 4. Circulation directions about jib and mainsail

The two-dimensional potential flow program (5) was used to study these effects and to present basic examples as to how the jib affects the mainsail and how the mainsail affects the jib. Again, viscous and separation effects were not included. However, basic potential flow results gave the understanding that was needed. The advantage of the CFD method over observing the real flow afloat was that the potential flow program could isolate and study each airfoil without the other being present and without the confusing effects of the boundary layer and separation. Streamline and pressure distribution plots from the CFD code gave the data necessary to correctly explain the jib-mainsail slot effect for the first time.

Effect of Mainsail on the Jib

Figure 5 shows the effect of the mainsail on the streamlines about the jib. The dotted line is the jib flow without the mainsail. The aft airfoil, the mainsail, causes an increase in the upwash flow coming into the jib. A large amount of air that originally flowed on the lower windward side of the jib now flows on the upper (lee) side. This matches our original view of the circulation about the two airfoils.

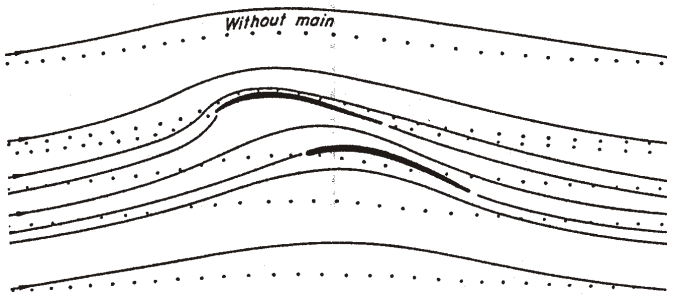

Figure 5. Effect of mainsail on jib streamlines.

Figure 6 shows the pressure distribution on the jib with and without the mainsail present as calculated by the potential flow program. The jib carries a much larger load with the mainsail present. However, another phenomena is present that is not so obvious from the simple circulation picture. The flow off the trailing edge of the jib (the leech) is faster with the mainsail present (the pressure is more negative). The Kutta condition is being satisfied on both airfoils by the potential flow program, but the dumping velocity at the trailing edge of the jib is determined by the combined flow of the jib and mainsail and it is higher. This phenomena is discussed in some detail by A.M.O. Smith (6) and also covered by C.A. Marchaj (7, p.635).

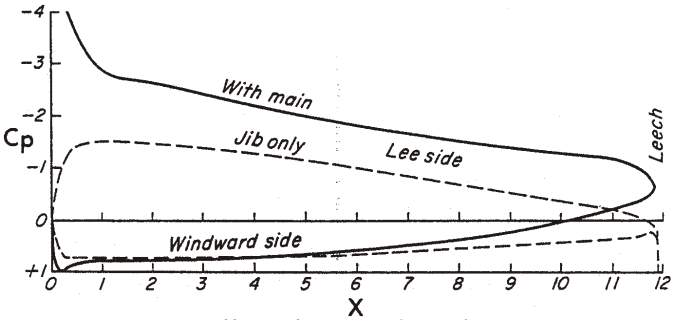

Figure 6. Effect of mainsail on jib pressures.

Effect of Jib on the Mainsail.

Figure 7 shows the streamlines about the mainsail with and without the jib. The jib reduces the upwash at the leading edge of the mainsail (the mast). Some of the air that passed between the headstay point and the mast will be forced to the lee side of the jib when both sails are present.

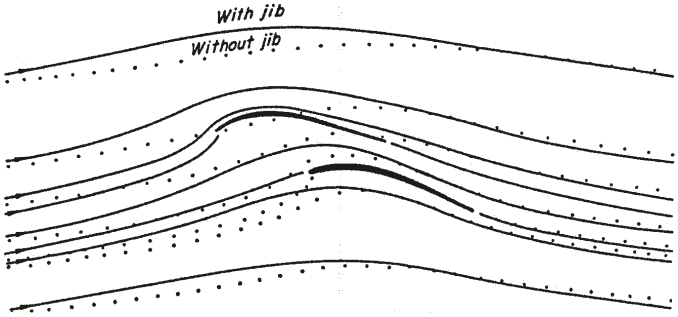

Figure 7. Effect of jib on mainsail streamlines.

Figure 8 shows the pressure distribution on the mainsail with and without the jib. Without the jib, the mainsail stagnation streamline is well onto the lower windward side of the sail. The flow accelerates around the mast and to the lee side of the mainsail producing high suction pressures followed by a rapidly increasing pressure. This adverse pressure gradient would cause the boundary layer to separate.

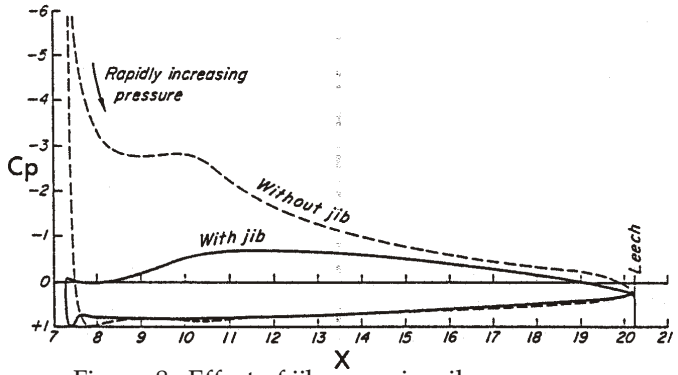

Figure 8. Effect of jib on mainsail pressures.

With the CFD code we can isolate the different physical aspects of the problem and determine just what causes what. The primary effect of the jib is that it reduces the suction pressures (and velocities) on the lee side of the mainsail. The potential flow efficiency of the mainsail is reduced by the jib. However, the real boundary layer is able to live with this revised lee-side mainsail pressure distribution without separating.

Note that the final trailing edge pressure on the jib (Figure 6) is higher than the mainsail trailing edge pressure. This is the result of the Kutta condition being imposed under the combined flow fields of both the jib and mainsail.

These explanations for the jib + mainsail flows were used by C.A. Marchaj (7,8) with the statement that they for the first time explained correctly the jib-mainsail interaction effect. The results were also used by P. Gutelle (9).

The Separation Bubble

Early CFD applications on thin aircraft airfoils required an understanding of the laminar separation bubble problem. As the angle of attack of the airfoil was increased the bubble grew, and under certain Reynolds numbers and angles it finally burst and the entire airfoil stalled. It occurred to the author that this same phenomenon might be present on the luff of thin sails, and this turned out to be the case. This led to the design of a series of short tufts placed end to end near the jib luff to measure the size of the separation bubble. This line of tufts is used differently than the long single telltale placed 12-18 inches from the luff on most jibs. With several short tufts in a row, the number of tufts twirling shows the size of the bubble and how the sail angle is changing between the stalling and the luffing condition (see Figure 9). Sailing experience proved that this special tuft system (or "Gentry verklikkers" as they are called in Holland) was very useful in windward sailing and sail trim (1-4, 7). Almost all of the l2-Meter yachts sailing in Australia in 1987 used this tuft system concept on their jibs.

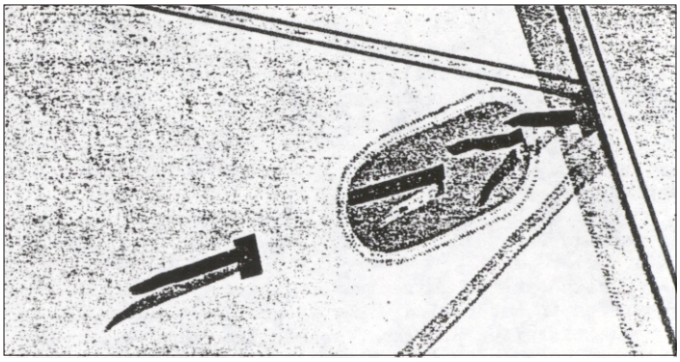

Figure 9. Tuft system to measure separation bubble.

Mast Design Aerodynamics

The same program used on the jib-mainsail interaction problem was used in 1974 to design a new mast for the America's Cup l2-Meter ***COURAGEOUS*** (10, 11). Studies with the potential flow program gave details of the mast design problem that could not easily be measured afloat. To support the analytical work, sailing tests were used to understand the separated flow regions and the effect of unsteady flow conditions.

It was important that the proper flow conditions were simulated in the CFD and in the sailing tests. The mast is the leading edge of the mainsail airfoil with its velocity and pressure distribution strongly influenced by the presence of the jib and the mainsail. Studies of the flow around a mast standing alone would be of no use.

Conventional non-rotating sailboat masts have a region of separated flow on the aft lee-side of the mast. In the analytical studies the area behind the mast where the flow is usually separated was smoothed over. Computer runs with the potential flow program and a separate boundary layer analysis showed that the amount of separation depended primarily on the condition of the boundary layer as it faced the first adverse pressure

gradient. This was verified by the sailing tests.

The initial design objective was to find a mast shape that would have reduced separation. From basic boundary layer theory it was clear that a turbulent boundary layer on the mast would reduce the amount of flow separation. The problem then became one of finding a mast section shape that would help trip the flow to the turbulent flow condition before it reached the first adverse pressure gradient.

A series of computer runs were made to determine how the pressure distributions changed with mast cross section shape. Some examples are shown in Figure 10.

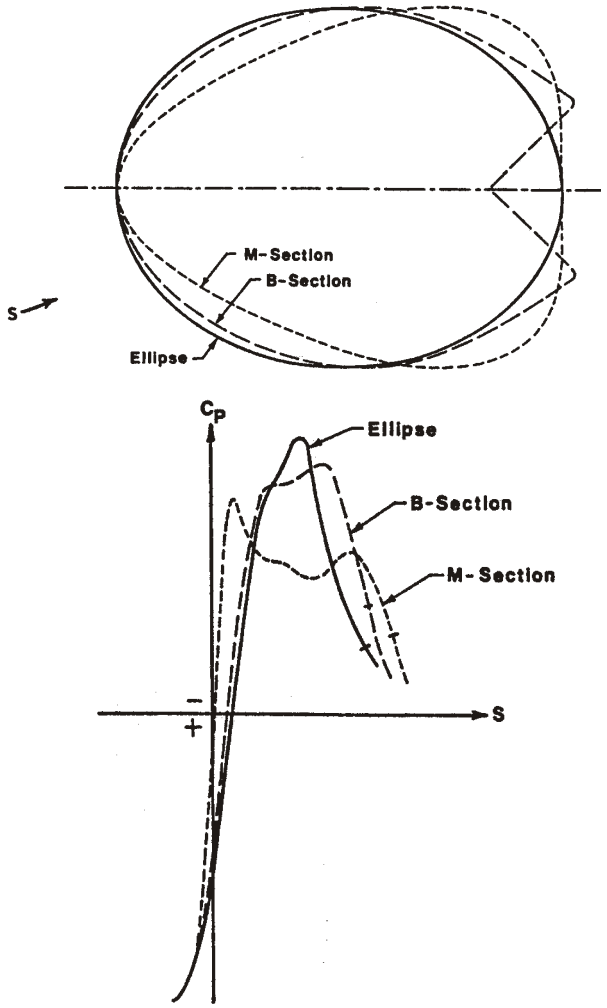

Figure 10. Shapes and pressure distributions of initial mast sections.

The cross sections were tried in short sections in live sailing tests. A variety of methods were used to visualize the flow during the tests including small tufts on the mast section and mainsail, soap bubble streams generated by a special nozzle driven by a small compressor, and a pressure rake. The condition of the boundary layer was studied with the use of a special surface paint that changed color depending upon the amount of ammonia present in the boundary layer (ammonia was pumped through small holes at the leading edge). The paint color changed from yellow to blue at the turbulent transition point. A thin-film gauge was also used to determine the effect of trip devices on the boundary layer transition.

The sailing tests indicated that the mast leeside separation matched the CFD calculated adverse pressure gradient location. In the sailing tests the M-section in Figure 10 had a separation point farther aft than the other sections. This led to the idea of developing a mast section shape that would have a long region of approximately flat pressure gradient prior to the start of the adverse gradient. This region of constant pressure (and constant speed) might provide sufficient running length for a boundary layer trip system to trip the flow to turbulent.

Numerous CFD analysis runs led to a shape with a flat-topped pressure distribution which had the dual purpose of giving sufficient length to trip the boundary layer, plus a higher leading edge thrust. The final shape is shown in Figure 11. Final full scale sailing tests verified that the new shape represented an improvement over previous mast sections.

This shape was used on the mast for ***COURAGEOUS*** in the 1974 and 1977 America's Cup defenses. A similar mast was designed and used on ***FREEDOM*** in the 1980 Cup races.

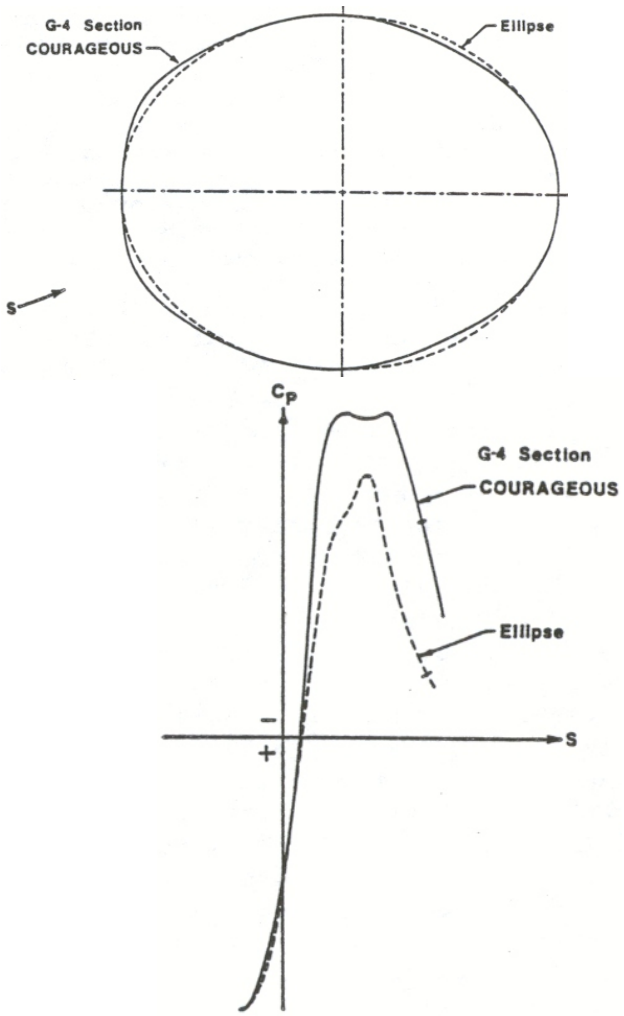

Figure 11. Final *Courageous* mast shape.

The author was asked to design a new mast for use on ***LIBERTY*** for the 1983 Cup defense and conducted some sailing tests on board ***FREEDOM*** in the summer of 1982. The mast and mainsail were tufted and observed under various sailing conditions. Photographs were taken of the sails and later digitized for input to the computer analysis.

The sailing tests indicated that the original mast design was excellent in smooth water but that the separation was a bit too sensitive to the dynamic motion of the boat in a seaway. A new mast section was designed for ***LIBERTY*** to improve this situation. This involved the use of a new multi-element airfoil program that had an inverse design capability (12). An initial shape was analyzed by the program and the pressure distribution plotted. A new desired pressure distribution was then sketched and input to the program and the code generated a new mast shape. The process was repeated several times until the desired results were achieved.

Experimental Studies of a Multi-Element Wing Sail

The material presented in the previous sections of this paper is a summary of work conducted by the author between 1969 and 1983 and involved only "soft" sails. CFD codes have improved since that time and it would be interesting to apply the latest programs available to the author to the type of sail that has been built by the *Sail America* syndicate for the 1988 defense of the America's Cup against the New Zealand 90-foot waterline challenger. The new *Sail America* boat is a 60 foot catamaran christened ***STARS & STRIPES*** and sports a solid multi-element wing for its sail power. (The legality of this boat as a cup defender was still being challenged by New Zealand in the courts as this is being written.)

It should be emphasized that the present author was not part of the ***STARS & STRIPES*** design team. The wing sail shape and the airfoils used in this paper were derived from photographs of the ***STARS & STRIPES*** and must be viewed as only rather crude approximations of the actual design. The airfoil shapes used in this exercise are probably far from optimum.

This provides an interesting situation for the application of CFD. The author is applying CFD to new problems for which he is completely unfamiliar and has no test data to verify any of the findings or conclusions. Also, the results presented were obtained in a very short period of time. Therefore, these data should be viewed more as a CFD experiment rather than as actual design data. However, the analysis steps presented are typical of how CFD would be used in the first stages of an actual design process. It will be interesting to eventually see how the results of this very brief CFD experiment match what is found on the actual sailing catamaran.

The ***STARS & STRIPES*** wing sail has a forward airfoil with an attached small movable tab. The aft airfoil has a slightly longer chord than the forward airfoil (at least over the lower part of the mast). There is a small slot between the forward and aft wing airfoils and of course, the airfoils are symmetrical. The wing camber is adjusted from one tack to the other by changing the angle between the forward and aft airfoils and adjusting the tab on the forward airfoil.

Several basic objectives were selected for this study of the wing sail:

1. Demonstrate that the basic theories described previously for thin soft sails also apply to the thick wing sail. In particular, show that the improvement on the aft airfoil is not due to any "high speed" flow in the slot "revitalizing" the aft airfoil boundary layer, but due to the fact that the forward airfoil suppresses the lee-side pressures of the aft airfoil.
2. Learn how the pressure distribution builds about the airfoils as the angle of attack is increased.
3. Study how the boundary layer behaves with different airfoil deflections and angles of attack.
4. Generate lift versus angle of attack data for two different camber shapes.
5. If possible, determine the airfoil stalling angles.
6. Apply a 3-dimensional panel method to the wing sail.

The CFD computer program selected for the two dimensional part of this study was a modified version of the Boeing multi-element airfoil program (12) recently completed by Wen-Fan Lin of the Boeing Aerodynamics Research Group. The program is basically a potential flow problem solver coupled with a viscous flow problem solver in an iterative fashion. That is, the inviscid flow is calculated by the potential flow solver and the results input to the boundary layer. The boundary layer solver furnishes the boundary layer displacement effect which is then fed back into the next inviscid solution. The process is continued until it converges.

The potential flow solver is based on a higher order panel method for two-dimensional airfoils. It can be run in either an analysis mode (direct) or in a design mode (inverse). Only the analysis mode was used in the results presented here. The design mode was, however, used in the design of the mast for ***LIBERTY*** as previously discussed.

The viscous problem solver uses a momentum integral approach to calculate the boundary layer characteristics. The integral boundary layer solver calculates the laminar boundary layer, laminar separation, the laminar separation bubble, transition based on a correlation of Granville, and the turbulent boundary layer. The turbulent calculations use the momentum integral method, a power law velocity profile, Garner's equation for the form parameter, and the Ludwieg-Ti11man equation for wall shear stress. The turbulent separation point is assumed to occur when the shape factor, $H = 2.8$. The program includes a simulation of any separated flow regions on the airfoils. The boundary layer displacement effect between iterations is accounted for using a transpiration method.

Basic Interaction of Multi-Element Wing Sail Airfoils

The basic principles of the interaction between the jib and mainsail as already outlined must also apply to the solid-wing sail airfoils. This fact will be illustrated in the following examples. However, with the new program that includes viscous and separation effects, we should be able to study the flow right up through the airfoil stall.

The solid wing is certainly much easier to simulate than the thin soft sails since it does not change its shape (luff) at the lower angles of attack. For all of these studies the wing angle of attack will be measured relative to the centerline of the forward wing airfoil. The aft airfoil angle will be measured relative to the forward wing centerline (the "flap" deflection angle). Since the wing sail has a wide range of angle adjustments relative to the true wind and since the boat spends most of its time either beating or close reaching, no attempt has been made in these studies to identify the angle that the wing sail system makes relative to the boat direction.

The dimensions of the airfoils studied are only approximate as they were taken from available photos of ***STARS & STRIPES***. For the two-dimensional studies the chord length of the forward airfoil was taken as 8.9 feet and the flap chord was set at 11.2 feet. All of the results presented are for a unit Reynolds of 0.265×10^6 which represents an apparent wind speed of 25 knots. The program was allowed to calculate its own transition and separation points.

The Boeing Aero Grid & Paneling System (AGPS) (13) was used to generate all the geometry data needed for input to the CFD code and for much of the output post processing.

The basic airfoils are shown in Figure 12. In this example the flap is deflected 20 degrees. Runs were made with both a zero and 10 degree tab rotation about the 80% chord point. Analysis runs were also made with a 5 degree tab and 10 degree flap combination. These angles are not optimum but were selected merely as typical starting points for the design process.

Inviscid results for the forward airfoil alone at zero angle of attack are shown in Figure 13. The inviscid results for the aft airfoil alone at its 20 degree deflection angle are shown in Figure 14. Note the very high pressure peak at the leading edge of the aft airfoil. Previous discussions indicate that the boundary layer will probably separate at the adverse pressure gradient, and that is exactly what the program tells us when we let it run for a number of inviscid/ viscous iteration cycles (Figure 15). The aft airfoil is clearly stalled without the forward airfoil.

When both airfoils are present, we get a different picture (Figure 16). The forward airfoil suppresses the peak pressure on the lee side of the aft airfoil. The boundary layer on the aft airfoil is able to handle this new pressure distribution, the air does not separate, and the airfoil is no longer stalled. The aft airfoil has a strong influence on the forward airfoil. Even though the forward airfoil is at zero angle of attack itself, the flow induced by the aft airfoil causes a strong upwash in the streamlines coming into the forward airfoil leading edge, and the front airfoil now generates considerable lift.

All of these effects are exactly as we would expect from the much earlier completely inviscid work on the jib-mainsail interaction problem. However, with a more sophisticated code that includes viscous and separation effects we are able to see the complete process in more detail.

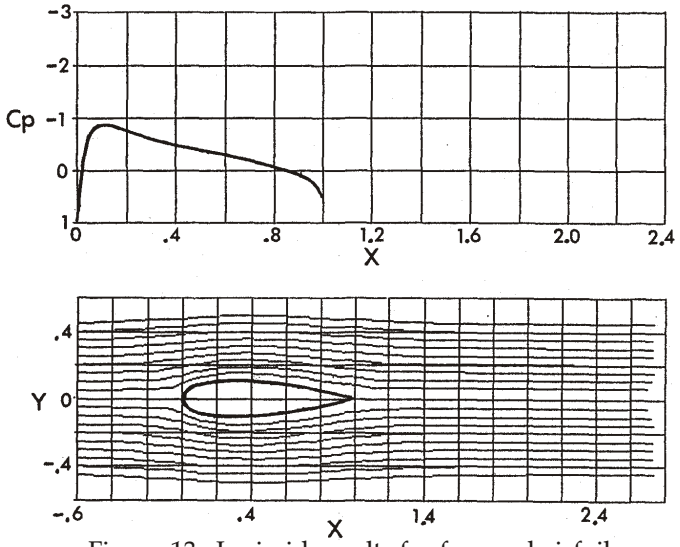

Figure 13. Inviscid results for forward airfoil.

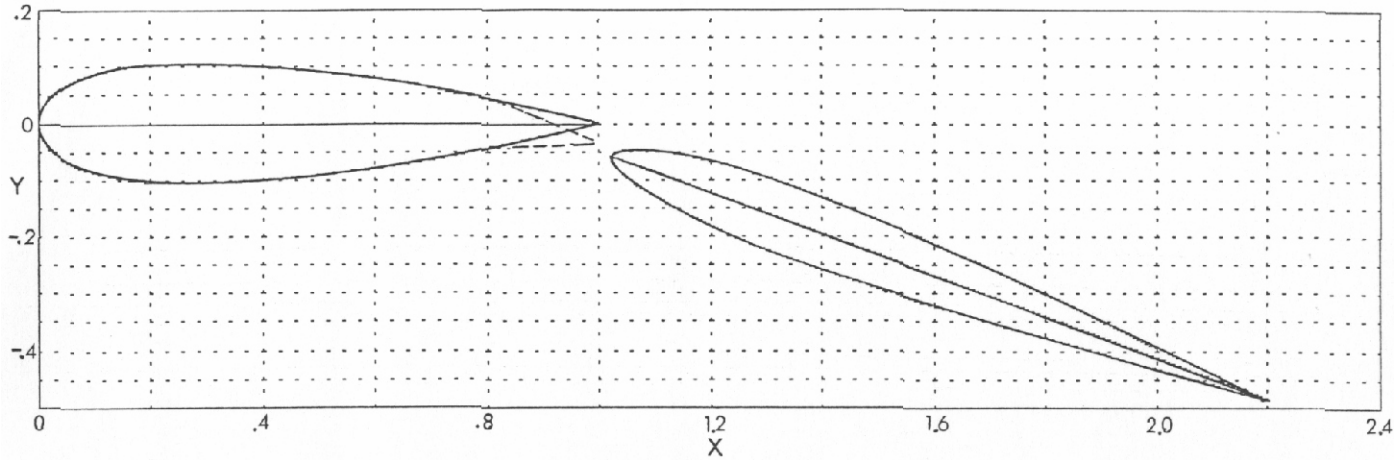

Figure 12. Experimental airfoils used for solid wing study.

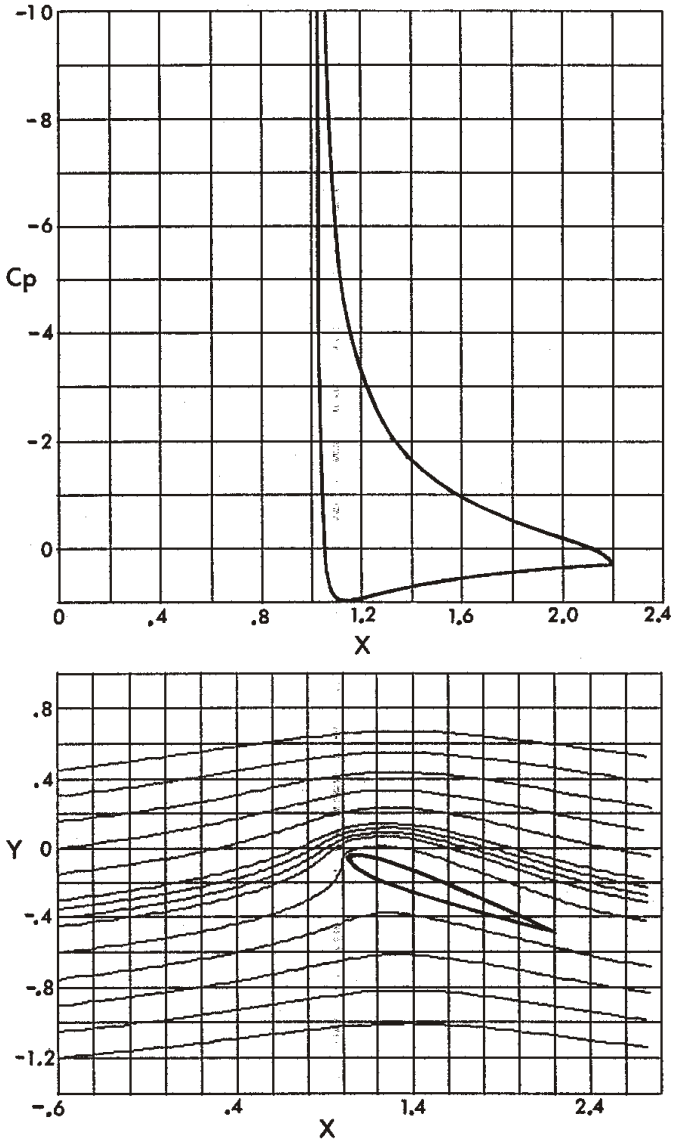

Figure 14. Inviscid results for aft airfoil only.

On a highly cambered single element airfoil, the boundary layer has a hard time withstanding the adverse pressure gradient over the entire length of the upper surface flow. With two airfoil components and a slot between, we have a much better design. The circulation fields about the two airfoils tend to cancel each other in the slot and the air slows down.

The peak pressure gradient on the aft airfoil is reduced by the presence of the forward airfoil. The boundary layer on the lee side of the aft airfoil is starting fresh at the stagnation point rather than having suffered through the adverse pressure gradient on the forward airfoil. The boundary layer on the aft airfoil is not "energized" by any high-speed slot flow. As with the jib-mainsail interaction, the load on the front airfoil is much higher because of the upwash due to the aft airfoil and because its trailing edge Kutta condition is satisfied in a higher speed region on the lee side of the aft airfoil.

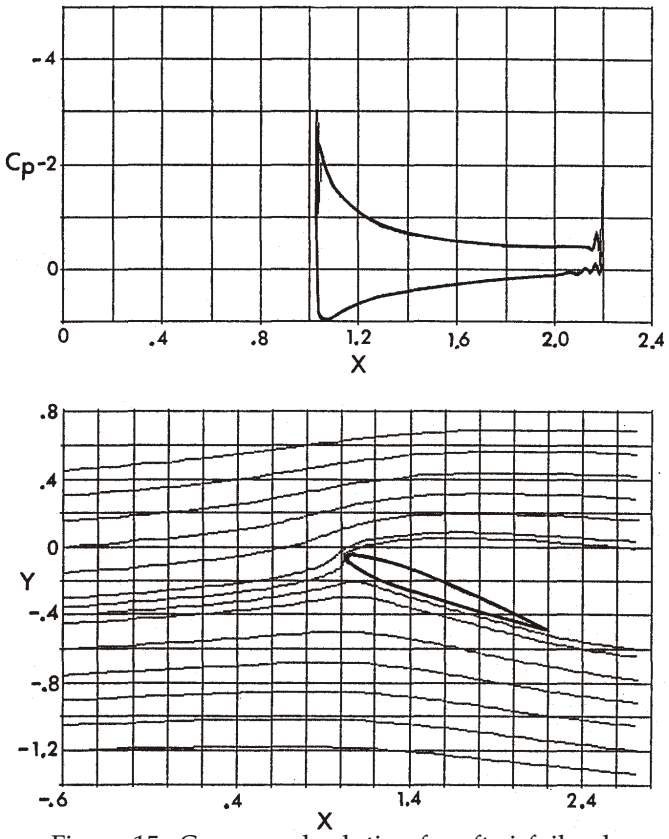

Figure 15. Converged solution for aft airfoil only.

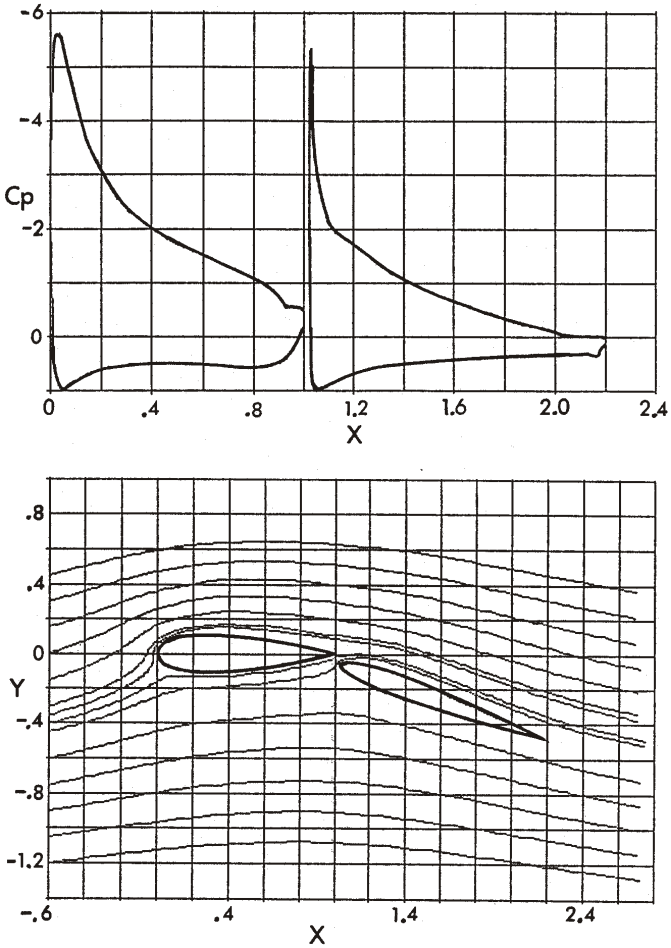

Figure 16. Converged solution for both airfoils.

The Inviscid / Viscous Convergence Problem

The CFD program used for this study calculates the inviscid and viscous flows using completely different sets of equations. Their interaction effects are accounted for by repeating the calculations through several iteration cycles. The basic problems with such an approach are; when is the flow converged, and does it converge to the correct solution?

A good example of the inviscid/viscous iteration process is shown in Figure 17. In this case the angle of attack was 12 degrees, the tab was deflected downward 10 degrees, and the flap was deflected 20 degrees to give a highly cambered configuration. On cycle one there is a peak velocity at the tab hinge point at X=0.8. In the next few cycles the flow is separated off of the tab. By the 6th and 7th cycles the separation has become stable at X=0.55. As the separation on the front airfoil moves forward it is not as efficient in suppressing the peak pressure on the aft airfoil, and the separation on the aft airfoil starts to move forward also.

One means of monitoring the convergence process is to watch the changes in the total lift coefficient, C_ℓ and the forward airfoil flow separation point. This is illustrated in Figure 18. However, some computer runs at high angles of attack were slow to converge. The separation point just slowly marched forward on the forward airfoil. This situation means that the airfoil is probably stalled, or will stall if enough cycles are run (once this was identified the case could be rerun with a flag set to force a more rapid forward movement of the separation point). A few other runs would converge to what was apparently the correct solution and then oscillate about that solution until the iterations were stopped. It is obvious that convergence plots must be made for every run to be sure that the solution converges properly and that the correct final solution is being selected from the iteration cycles.

Prediction of Airfoil Stall

A series of runs were made to see if the CFD method could calculate the airfoil stall point. The results are presented in Figure 19. Two different tab/flap angle combinations were studied to see how total effective camber influenced C_ℓ and the stall. The tab and flap angles were selected quite arbitrarily and may not represent what is actually used on the real catamaran.

At 16 degrees angle of attack for both configurations the final flow separation point was close to the leading edge of the forward airfoil and at about the midpoint on the aft airfoil. The calculated C_ℓ's had also dropped off sharply at 16 degrees.

Considerable separation was also already present on both systems at 12 degrees angle of attack. For the 20 degree flap system the converged separation point was at X=0.5l on the upper surface of the forward airfoil. The 10 degree flap system had a converged separation point at X=0.66. Computed streamlines are shown in Figure 20 at 8 degrees angle of attack for the tab=5, flap=10 camber

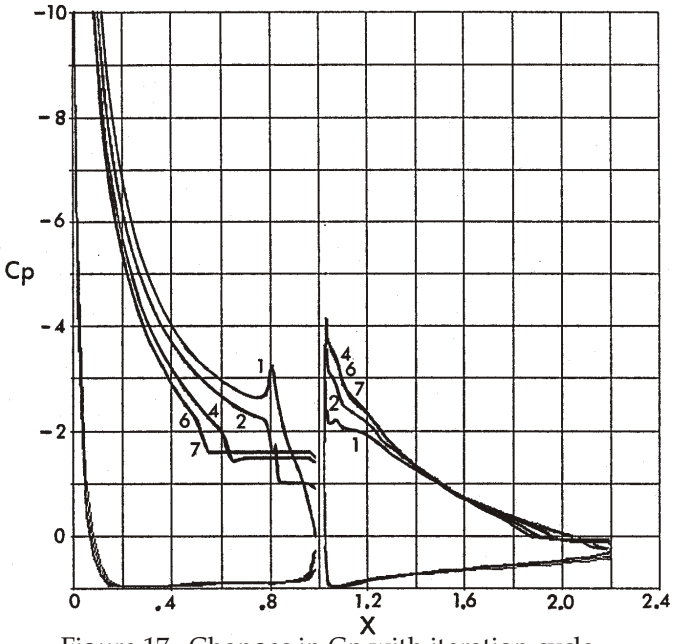

Figure 17. Changes in Cp with iteration cycle.

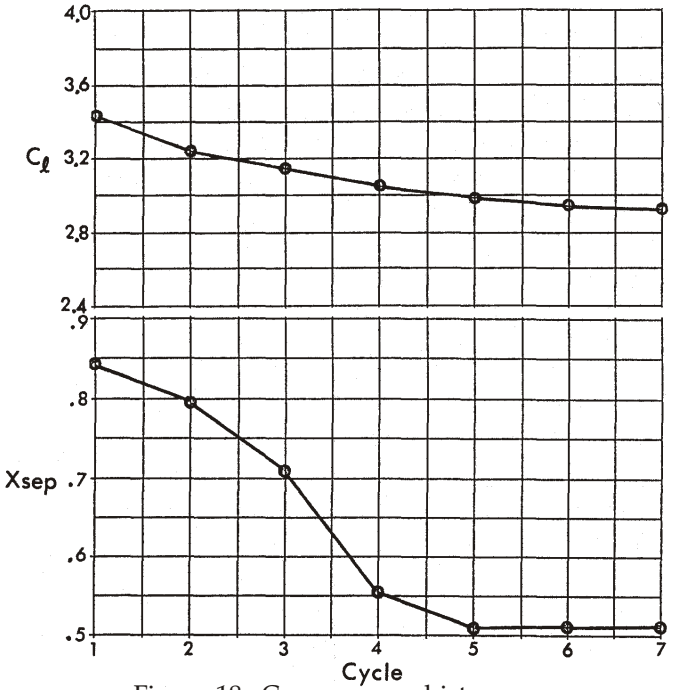

Figure 18. Convergence history.

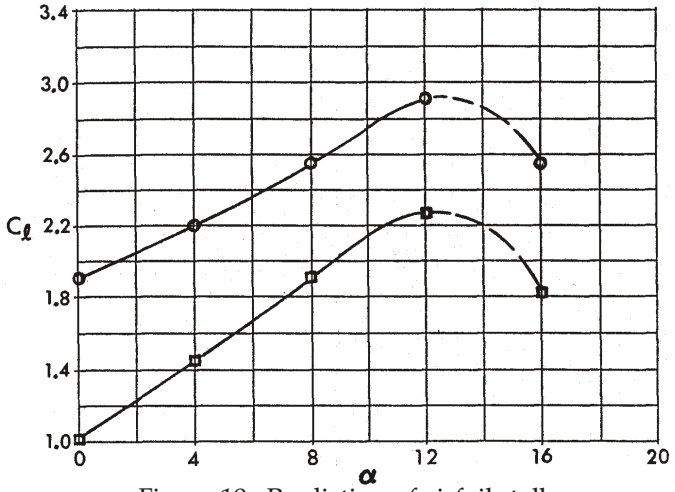

Figure 19. Prediction of airfoil stall.

condition.

At zero degrees angle of attack the flow on both camber configurations was unseparated except for the tab region on the forward airfoil. These results indicate that tab deflections of 10 degrees for the 20 degree flap case and 5 degrees for the 10 degree flap case might be too high. This suggests that the flow on the tab on the real catamaran should be watched carefully with the aid of several rows of very short tufts. Longer conventional telltales on the tab might not show the actual tab separation.

For these calculations the program input freestream turbulence level was set to zero. The transition was left free to be calculated by the program. Changes in these assumptions would probably give different output results.

Wing-Sail Thrust-Drag Loops

The term "lift" is normally defined as a force perpendicular to the freestream velocity vector. How much of this force is available to produce forward boatspeed depends upon the angle that the boat centerline makes with the wing sail reference line and the direction of the freestream velocity vector. The integration of the pressures on the sail in a direction perpendicular to the boat centerline gives the boat driving force. This "thrust-drag loop" method is useful in understanding the driving force generated by the wing sail. A sample thrust-drag plot for a 30 degree angle is shown in Figure 21 for the 10 degree flap deflection case. In this case both airfoils are producing forward thrust. At lower angles the forward airfoil produces almost all of the thrust with the aft airfoil serving the purpose of loading up the forward airfoil.

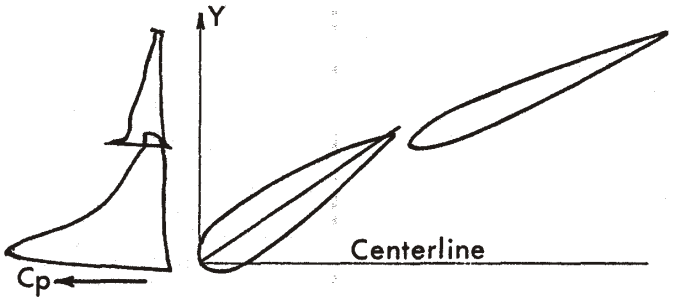

Figure 21. Thrust-Drag loops

Three-Dimensional Effects

All of the results presented to this point have been based on two-dimensional analysis. One reason for this is that the solid-wing sail has a high aspect ratio so the 2-D results should be close to the real physical flow. Also, the 2-D method included iterative viscous and separation effects. However, a 3-D inviscid analysis should shed light on root and tip effects plus give some idea of the efficiency of the wing from the span-load distribution standpoint. For this study the direction of the freestream velocity vector was assumed to be constant and was not varied spanwise along the wing as would be the situation on the real boat.

The 3-D panel method used for these calculations was the Boeing PAN AIR Technology code (identified as Boeing program A502). This program was selected because of its many capabilities and because it is available for general use by the public (14).

Program A502 solves the general three-dimensional aerodynamic/hydrodynamic problem for arbitrary configurations. The program uses a higher-order panel method based on the solution of the linearized potential flow boundary-value problem. Results from A502 alone are not usually applicable to cases where viscous effects and separation are dominant. Viscous results can be obtained using a separate 3-D finite difference boundary layer program. However, time was not available to include 3-D boundary layer results for this study.

The A502 panel geometry used for this study is shown in Figure 22. The aft airfoil of the real wing is broken into a number of flap sections so that twist and camber can be adjusted spanwise. For simplicity this study used a smooth variation of the angle of the flap from 20 degrees at the root to 10 degrees at the tip. The airfoil sections were the same as used for the 2-D analysis except that the forward airfoil tab deflection was zero.

The 3-D geometry and paneling were generated using the Boeing Aero Grid and Paneling System, AGPS (15). The wing root airfoil was assumed to be 5.4 feet off the water which was taken as the reflection plane. The wing was represented by 1,434 panels plus a wake system extending downstream. The A502 program was run on a Cray X-MP computer.

The span load calculated by the A502 program is shown in Figure 23. The gap between the wing root and the reflection plane (the water) causes a rapid loss in load on the lower part of the wing. Some sort of wing root end plate would help this situation if a practical design could be made.

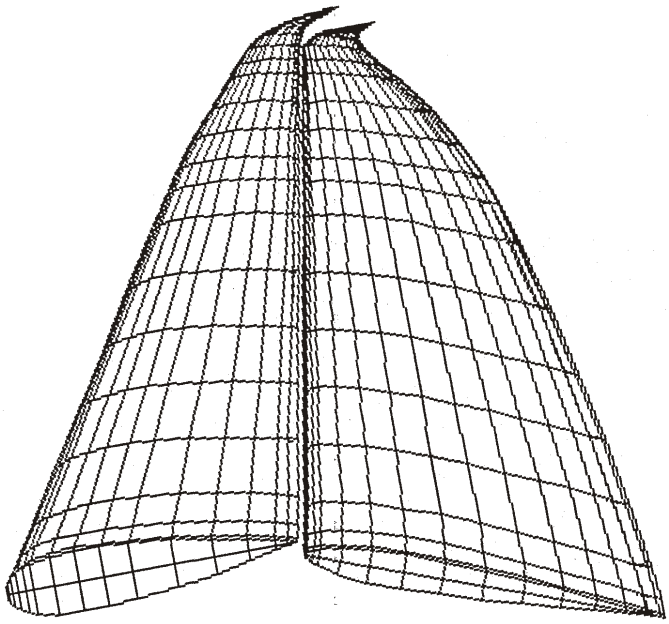

Figure 22. Wing paneling used for A502 program.

Detailed results for the zero angle of attack case are shown in Figure 24 on Page 12. The data presented include pressure distributions at se1ected wing stations and constant pressure contour lines for the top (leeward) and bottom (windward) surfaces of the wing. The pressure contour plot originals are in color and give a quick view of the three-dimensional aspects of the flow.

Conclusions

Although the computational fluid dynamic tools used in these studies were developed only for aircraft design purposes, they are capable of providing useful results when applied to a variety of sail aerodynamic problems. These tools led to the development of the correct explanation for the jib-mainsail slot effect and to the discovery and use of the laminar separation bubble for windward sailing. Mast sections developed using CFD were used on the America's Cup defenders ***COURAGEOUS*** (1974 & 1977), ***FREEDOM*** (1980) and ***LIBERTY*** (1983).

An experimental study of the use of both two dimensional and three-dimensional CFD methods has indicated that such tools probably would be useful in the design process for solid-wing sails such as those being used on modern high technology catamarans.

The basic problems in applying CFD to sails are about what one would expect; the tools were developed for aircraft and sometimes do not contain certain capabilities needed in the analysis of sails. For example, the standard programs do not provide a means for changing the freestream velocity vector to represent wind shear from the deck to the top of a sail.

A basic problem exists in that the sailor is able to change the shape of his sails to match the real airflow conditions and the computer cannot. The CFD programs require that the complete sail shapes be input at the beginning of the solution. Providing shapes that match both realistic sailing conditions, plus what the CFD program sees, is a difficult task. This is particuu1ar1y true when attempting to model thin "soft" sails but also applies to the wing sail.

Acknowledgments

This paper was prepared as a research project under the Flight Research Institute (FRI), Seattle, Washington. Approval to use the Boeing CFD codes and access to the necessary computer time was arranged through the FRI.

The author is indebted to Wen-Fan Lin of the Boeing Aerodynamics Research Group for his guidance on the use of his new version of the Boeing 2-D Multielement Airfoil Program, and to Jim Thompson for his photographs of the new ***STARS & STRIPES*** catamaran.

This paper is dedicated to the memory of David K. Snepp, who lived life with style, courage, and a great sense of humor.

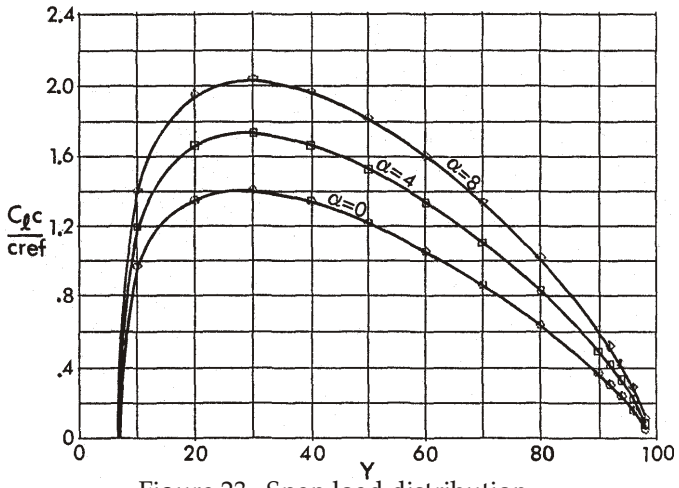

Figure 23. Span load distribution.

References:

1. Gentry, A.E., How Sails Work, *SAIL* Magazine, April 1973 thru January 1974.
2. Anthology, The Best of SAIL Trim, *SAIL* Books, Inc., 1975.
3. Gentry, A.E., The Aerodynamics of Sail Interaction, Ancient Interface III, The 3rd AIAA Symposium on Sailing, Nov. 20, 1971, Redondo Beach, Calif.
4. Gentry, A.E., A Review of Modern Sail Theory, The Ancient Interface XI, 11th Annual AIAA Symposium on Sailing, Sept. 12, 1981, Seattle, Washington.
5. Giesing, J.P., Potential Flow About Two-Dimensional Airfoils, McDonnell Douglas Report NO. LB-31946, December 1965.
6. Smith,A.M.O., High Lift Aerodynamics, AIAA Paper No 74-939, Los Angeles,1974.
7. Marchaj, C.A., Aero-Hydrodynamics of Sailing, Dodd, Mead & Company, New York, 1979.
8. Marchaj., C.A. Sailing Theory and Practice, Revised, Dodd, Mead & Company, 1982.
9. Gutelle, P., The Design of Sailing Yachts, International Marine Publishing Company, Camden, Maine, 1979 (from the French edition).
10. Gentry, A.E., Studies of Mast Section Aerodynamics, The Ancient Interface VII, 7th Annual AIAA Symposium on Sailing, Jan. 31, 1976, Long Beach, California.
11. Gentry, A.E., Design of the COURAGEOUS Mast, Yachting Magazine, Feb. 1975.
12. Henderson, M.L.; A Solution to the 2-D Separated Wake Modeling Problem and Its Use to Predict Maximum Lift Coefficient of Arbitrary Airfoil Sections." AIAA Paper No. 78-156, Jan. 1978.
13. Snepp, D.K., & Pomeroy, R.C., A Geometry System for Aerodynamic Design, AlAA-87-2902, AIAA/AHA/ASEE Aircraft Design, Systems and Operations Meeting, St. Louis, Missouri, Sept. 1987.
14. Saaris, G.R., A502F User's Guide PAN AIR Technology Program for Solving Problems of Potential Flow about Arbitrary configurations, Boeing Report D6-538l8, June 1987.

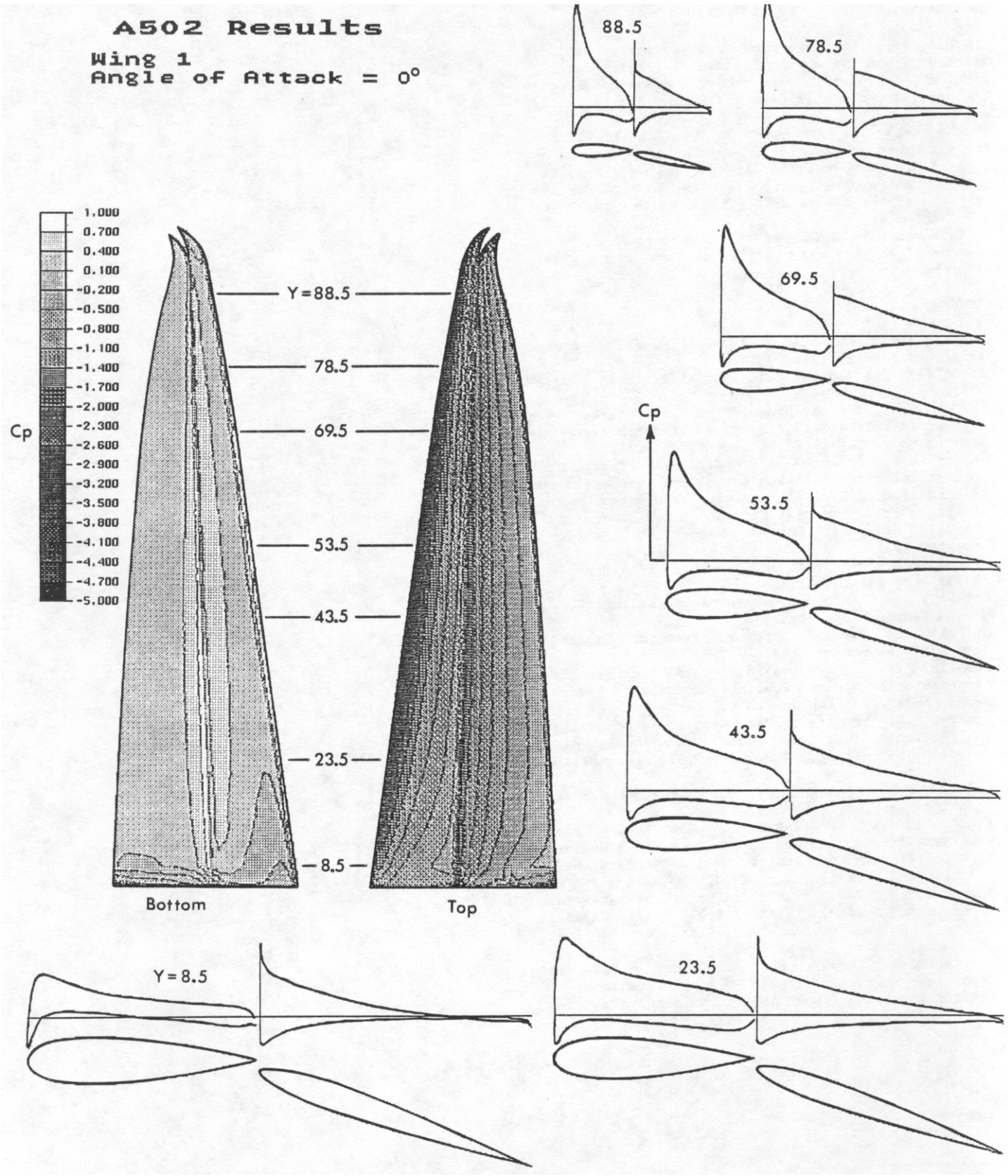

Figure 24. A502 results for the solid wing.